Oxidation of the Two β-Carotene Molecules in the Photosystem II Reaction Center†

Alison Telfer,‡ Dmitrij Frolov,§ James Barber,‡ Bruno Robert,§ and Andy Pascal*,§

Wolfson Laboratories, Department of Biological Sciences, Imperial College of Science, Technology and Medicine, London SW7 2AY, U.K., and Service de Biophysique des Fonctions Membranaires, DBJC/CEA and URA 2096/CNRS, CEA-Saclay, 91191 Gif-sur-Yvette Cedex, France

Received May 28, 2002; Revised Manuscript Received December 3, 2002

ABSTRACT: We present a spectroscopic characterization of the two nonequivalent β-carotene molecules in the photosystem II reaction center. Their electronic and vibrational properties exhibit significant differences, reflecting a somewhat different configuration for these two cofactors. Both carotenoid molecules are redox-active and can be oxidized by illumination of the reaction centers in the presence of an electron acceptor. The radical cation species show similar differences in their spectroscopic properties. The results are discussed in terms of the structure and unusual function of these carotenoids. In addition, the attribution of resonance Raman spectra of photosystem II preparations excited in the range 800−900 nm is discussed. Although contributions of chlorophyll cations cannot be formally ruled out, our results demonstrate that these spectra mainly arise from the cation radical species of the two carotenoids present in photosystem II reaction centers.

Carotenoids (Car)[1] serve two vital functions in almost all photosynthetic proteins. They are antenna pigments, augmenting the light-harvesting capacity of the system via singlet−singlet excitation energy transfer (*1*). Second, they perform a protective function, quenching chlorophyll triplets (^{3}Chl) formed by intersystem crossing before the latter can interact with triplet oxygen to give its very reactive singlet form, $^1O_2$ (*2*, *3*). Both of these functions (light-harvesting and triplet quenching) require a close proximity between the carotenoid and chlorophyll molecules (see refs *1* and *4*). Carotenoids are obligatory in oxygenic photosynthetic organisms due to their protective function. Moreover, in carotenoid-less mutants of anoxyphotobacteria, exposure to light in the presence of oxygen results in an intense photooxidative stress for these organisms, resulting in the appearance of revertant strains able to perform carotenoid biosynthesis (*5*). In all photosynthetic proteins (aside from those in carotenoid-less mutants) whose structure is resolved to sufficient detail, the distance between carotenoid, and at least some of the (bacterio)chlorophyll is only a few Angstroms (e.g., *6*−*9*).

The PSII reaction center (RCII) consists of the two main polypeptides, D1 and D2, along with a number of smaller ones including the α and β subunits of cytochrome b_{559}. In vivo, this PSII subcomplex binds all of the cofactors involved in its role as a water−plastoquinone oxido-reductase. It is now generally accepted that the isolated RCII binds up to 6 Chls *a*, 2 pheophytins *a*, 2 β-carotenes, and the heme b_{559} (*10*−*12*). However, the two tyrosine electron donors (Y_Z and Y_D) are inactivated, and the two bound quinone electron acceptors (Q_A and Q_B) are lost (*13*). Thus, in the absence of an external electron acceptor, this preparation is only capable of performing reversible charge separation. The D1 and D2 polypeptides are related to the L and M subunits of the reaction center of purple photosynthetic bacteria, the structure of which was resolved to atomic resolution over 10 years ago (*14*). Recently, the structure of an oxygen-evolving PSII core complex has been determined to a resolution of 3.8 Å by X-ray crystallography (*15*). Although a number of features can be observed in this structure (including the majority of its redox-active components), it is not yet precise enough to resolve any of the carotenoid molecules bound to the complex. The two β-carotene molecules present in RCII can be distinguished from each other as they exhibit different electronic properties. Dichroism measurements indicate that Car_{507} displays absorption transitions at 507, 473, and 443 nm and is nearly parallel to the membrane plane, while Car_{489} (peaking at 489, 458, and 429 nm) is approximately perpendicular to it (*16*−*19*). It should be noted that, although many RCII preparations have less than two Cars per center, the removal of these spectroscopically distinct species is nonselective (see refs *12* and *20*).

In isolated RCII, low-efficiency singlet−singlet energy transfer (20−25%) is observed from these two β-carotene molecules to Chl (*16*−*19*, *21*), but they exhibit essentially no ^{3}Chl quenching (*22*, *23*). Whereas the triplet state quantum yield of the primary donor ^{3}P680, formed via recombination of the primary radical pair $P680^{+\bullet}/Pheo^{-\bullet}$, is around 30% at room temperature that of ^{3}Car is less than 3%. The lifetime of ^{3}P680 shortens from 1 ms under anaerobic conditions to ∼30 μs in the presence of oxygen (*23*, *24*), and the $^1O_2$ thus

† This work was in part funded by an Alliance Franco-British Partnership Program. A.T. was in receipt of an EMBO short-term fellowship, and D.F. was supported by a Marie Curie Training Site grant. J.B. thanks the BBSRC for financial support.

* Corresponding author. Tel.: +33-169089015; Fax: +33-169084389; E-mail: apascal@cea.fr.

‡ Imperial College of Science, Technology and Medicine.

§ CEA-Saclay.

[1] Abbreviations: Car, carotenoid; Chl, chlorophyll; DM, n-dodecyl-β,D-maltoside; OD, optical density; P680, primary donor of PSII; PSII, photosystem II; Q_A and Q_B, quinone electron acceptors of PSII; RCII, reaction centre of PSII; SERDS, shifted-excitation Raman difference spectroscopy; SiMo, silicomolybdic acid ($SiMo_{12}O_{40}^{4-}$); Y_Z and Y_D, tyrosine electron donors of PSII.

10.1021/bi026206p CCC: $25.00
Published on Web 01/07/2003

produced causes severe damage to the pigment and amino acid moieties present (*25*, *26*). The Cars do, however, provide some protection against such "acceptor-side" photoinhibition (*27*) by diffusion-limited direct quenching of the $^1O_2$ formed (*28*).

The reason for the large distance of these Cars from the primary donor P680 lies in the extremely high oxidative power of the latter species, which is required to extract electrons from water. The redox potential of the couple $P680^{+\bullet}$/P680 is >1.1 V (*29*), and it is therefore capable of oxidizing any molecules of Chl *a* ($E_m \sim 0.8$ V; *30*) or β-carotene ($E_m = 1.06$ V; *31*) near to it. Thus, the Cars cannot be bound close enough to P680 to transfer singlet energy directly to it or to quench its triplet state, as they would also be able to donate electrons to $P680^{+\bullet}$ very rapidly and hence prevent normal functioning of the enzyme. When PSII is fully functional, the $P680^{+\bullet}$ species is reduced by a nearby tyrosine residue Y_Z, which in turn accepts electrons from the manganese atoms of the oxygen-evolving complex; a second, symmetry-related tyrosine, Y_D, can also be oxidized by $P680^{+\bullet}$ at a slower rate (*32*). In situations where donation from these tyrosine residues is inhibited (e.g., *33*), $P680^{+\bullet}$ can induce the oxidation of PSII-bound Car and/or Chl molecules despite the distance from it of the latter cofactors (*33*, *34*). Oxidation of β-carotene in isolated RCII occurs on a microsecond time scale (*35*), suggesting a distance of at least 17 Å from the oxidizing species (*36*) according to the Moser−Dutton rule (*37*). Consistent with this distance, and in order to permit the limited singlet energy transfer to Chl that is observed, Telfer (*20*) has proposed that these Cars are near to the two peripheral Chls, designated by Zouni et al. (*15*) as $Chlz_{D1}$ and $Chlz_{D2}$. Note that one or both of these chlorophyll molecules corresponds to the redox-active chlorin species termed Chl_Z (*38*; see Discussion section).

While both Car molecules can be photo-oxidized in RCII, the biphasic kinetics of irreversible bleaching appear to indicate that one is more readily oxidized than the other (*39*). Production of the cationic species $Car^{+\bullet}$ has been detected in various PSII preparations by an absorption increase around 990 nm (*33*, *35*, *40*−*43*). In experimental conditions where $Car^{+\bullet}$ persists, it is relatively unstable and becomes irreversibly bleached (*35*, *39*). The $Car^{+\bullet}$ radical(s) can, however, be rereduced via a pathway which may involve both chlorophyll and cytochrome cofactors (*33*, *34*, *38*, *44*), and this short-circuiting of electrons around PSII is believed to protect the system from "donor-side" photoinhibition, caused by oxidation reactions of $P680^{+\bullet}$ (*27*). The role of β-carotene in the PSII RC has been reviewed recently by Tracewell et al. (*45*) and Telfer (*20*). In this communication we will concentrate on properties of these two, nonequivalent β-carotene molecules in RCII, in both their neutral and cationic states.

MATERIALS AND METHODS

PSII-enriched membranes were isolated from market spinach (*46*) and frozen at −80 C until use. PSII RCs were isolated from these membranes by the method of De Las Rivas et al. (*39*) with the following modifications. The detergent digestion was carried out at 0.87 mg Chl/mL using 5% Triton X-100 for 2 h, with gentle stirring in the dark at 4 C. The first column chromatographic step (DEAE Toyappearl 650S, TSK) was performed in 0.25% Triton X-100, 50 mM Tris-Cl pH 7.2. PSII RCs were eluted with a 40−400 mM NaCl gradient in the same buffer. RCII-rich fractions were combined and frozen, as above, before further use. The PSII RC was further purified, concentrated and exchanged into 2 mM n-dodecyl-β,D-maltoside (DM), 50 mM Tris-Cl pH 7.2 on a small anion-exchange column (DEAE Toyappearl 650S, TSK). Prior to use, the PSII RC were finally concentrated further, desalted, and exchanged into 2 mM DM, 50 mM HEPES, pH 7, using Centricon 100 K cutoff concentrating tubes to a concentration of >200 OD at 675 nm (~2 mg Chl/mL). Cation production in the presence of SiMo (see below) was achieved by low-temperature illumination for ~20 min using white light from a Flexilux fibroptic illuminator (*42*).

Electronic absorption spectra were collected using a Varian Cary E5 double-beam scanning spectrophotometer. Samples at 20 μg Chl/mL were maintained at low temperature in a Helium bath cryostat (Maico Metriks, Tartu, Estonia) in 60% (v/v) glycerol, 2 mM DM, 50 mM HEPES, pH 7.2, with 2.5 mM SiMo as electron acceptor (~600 mol/mol RCII), plus an enzymic oxygen trap (5 mM glucose, 0.1 mg/mL catalase, 0.1 mg/mL glucose oxidase). Samples for resonance Raman measurements were concentrated to >200 OD at 675 nm, and an oxygen trap was added as described above; when required for cation production, SiMo was also added to around 40−50 mol/mol RCII (~15 mM SiMo for RCII at 200 OD). Raman spectra were recorded on a Jobin-Yvon U1000 double monochromator Raman spectrophotometer, equipped with an N_2-cooled, back-thinned, ultrasensitive charge-coupled-device detector (Spectrum One, Jobin-Yvon, France), on samples maintained at 77 K in an SMC-TBT nitrogen-flow cryostat (Air Liquide, France). Excitations in the blue and blue-green range were provided by Innova Argon and Krypton lasers (488.0, 496.5, 514.5, and 413.1 nm, respectively; Coherent, Palo Alto) and in the near-infrared range (700−900 nm) by a Titanium-Sapphire laser (Spectra Physics, model 3900S). Absorption spectra were taken before and after Raman measurements to verify sample integrity.

RESULTS AND DISCUSSION

Low-temperature illumination of PSII reaction centers in the presence of an electron acceptor results in a dramatic alteration of their absorption properties, due to the oxidation of a number of pigment cofactors (Figure 1; see also ref *42*). The most obvious of these spectral modifications is a partial bleaching of the Q_y electronic transition of RCII-bound Chl molecules, due to the production of a number of $Chl^{+\bullet}$ radical species that may include $Chl_Z^{+\bullet}$ and $P680^{+\bullet}$. These absorption changes were similar to those reported earlier (*47*). At the same time, significant bleaching occurs in the blue-green region of the absorption spectrum, where carotenoid molecules contribute. From inset a to Figure 1, it can be seen that the majority of this bleaching primarily affects the transitions of Car_{507}, at 507 and 473 nm. The electronic transitions of Car_{489} (489 and 458 nm) are also affected by illumination but to a lesser extent (~30% of the total carotenoid bleaching). The Q_x electronic transition of the pheophytin molecules at 543 nm is also perturbed, although this effect is mostly a band-shift rather than a true bleaching. Production of the $Car^{+\bullet}$ radical results in the appearance of

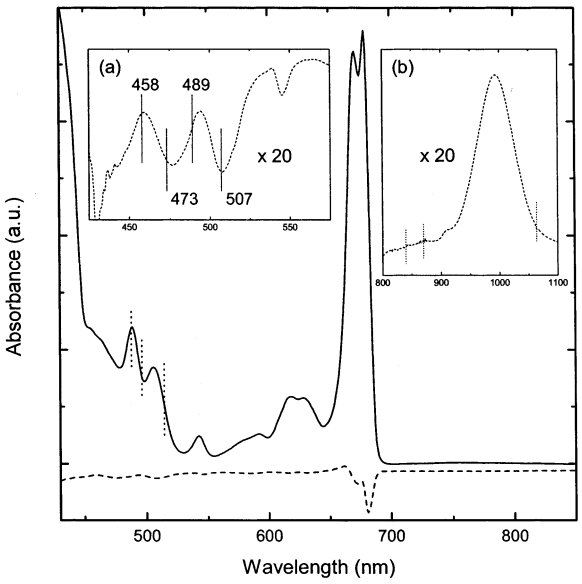

FIGURE 1: 20 K absorption spectrum of PSII reaction centers (solid lines), along with the corresponding difference spectrum induced by 20 K illumination in the presence of SiMo (dashed lines). The 425−575 and 800−1100 nm regions of the difference spectrum are shown enlarged in the insets (a and b, respectively). Dotted lines at 488.0, 496.5, 514.5, 840, 870, and 1064 nm indicate the positions of the laser lines used for Raman measurements.

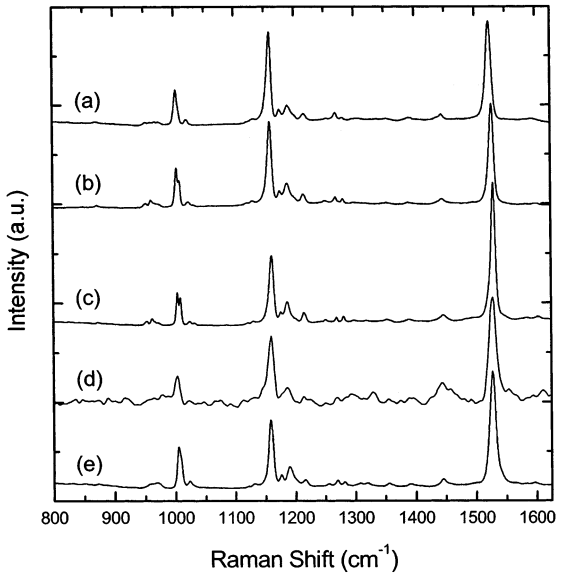

FIGURE 2: 77 K resonance Raman spectra of the neutral carotenoids bound to RCII (in the absence of SiMo), excited at 514.5, 496.5, 488.0, and 1064 nm (a−d, respectively). Also shown is a spectrum of isolated β-carotene in pyridine, excited at 496.5 nm (e).

a broad absorption band around 985−995 nm, while $Chl^{+\bullet}$ absorbs in the 820−850 nm region (Figure 1b; *33*, *34*, *42*).

Resonance Raman spectra of the neutral Cars bound to RCII in different excitation conditions are presented in Figure 2, along with a spectrum of isolated β-carotene in pyridine. These traces exhibit bands in the four main regions observed in carotenoid Raman spectra, called $\nu_1-\nu_4$ (around 1530, 1160, 1000, and 950 cm^{-1}, respectively; see Figure 2). As extensively discussed by Ruban et al. (*48*, *49*), when carotenoids exhibit different absorption properties, it is possible to extract their individual contributions by comparing Raman spectra obtained in different excitation conditions. Indeed, clear differences are seen between Raman spectra at different excitation wavelengths, which affect the position of the ν_1 (1523 cm^{-1} at 514.5 nm, 1529.5 cm^{-1} at 488.0 nm) and ν_3 (1002.5 cm^{-1} at 514.5 nm, 1004 and 1008.5 cm^{-1} at 488.0 nm) bands. Note that no such excitation-dependent differences, including splitting of the ν_3 band, are observed for isolated β-carotene in a number of solvents (e.g., Figure 2e). It may thus be concluded that these differences arise from the presence of the two carotenoid molecules in RCII, which exhibit slightly different resonance Raman spectra. Similarly, the ν_4 region, which is very sensitive to the precise configuration of the carotenoid molecule (*48*), also shows markedly different structure according to the excitation used, appearing somewhat more intense at lower wavelengths. Spectra obtained at 514.5 nm excitation (Figure 2a) are expected to be dominated by contributions from Car_{507}, while those of Car_{489} should become significant for excitations further to the blue. Excitation at 488.0 nm should result in strong resonance with Car_{489}, being at the peak of its 0−0 absorption transition. It is also, however, only 19 and 15 nm from the 0−0 and 0−1 transitions of Car_{507} respectively, and so contributions of the latter carotenoid are also expected to be significant. Spectra obtained in these excitation conditions indeed appear to contain contributions from two populations of carotenoid, as indicated by, for instance, the obvious splitting of the ν_3 band (Figure 2c). Also shown for comparison, in Figure 2d, is a spectrum excited at 1064 nm, in far preresonance conditions with both carotenoid molecules (cf. ref *42*). This excitation is located far from the electronic transitions of both carotenoids, and as expected, Raman spectra obtained in these conditions contain equal contributions from both Car_{507} and Car_{489} (note position of ν_1 and ν_3). Overall these spectra demonstrate that the two RCII-bound β-carotenes are in significantly different environments and/or configurations, consistent with the differences seen in their electronic properties (*16*−*19*).

These wavelength-dependent differences in the resonance Raman spectra are quite small, although significant, and it is not easy to relate them directly to differences in structural and/or functional properties of the two β-carotene molecules. The spectra are very similar to those published previously (*50*, *51*) and are consistent with these authors' conclusion of an all-trans conformation for both Cars. Evidence from HPLC pigment analysis has been presented for a 15-cis conformation of RCII-bound carotenoids (*52*), although this conclusion has since been challenged (*53*). Note that no trace of 15-cis Cars could be observed in our spectra (Figure 2)—in particular, the absence of the characteristic band around 1245 cm^{-1} (*54*, *55*). The increase in intensity of the ν_4 band relative to ν_3 with 488.0 nm-excitation indicates that Car_{489} is somewhat more distorted than Car_{507} (*56*).

To investigate the cations produced upon illumination of RCII particles, it is first necessary to estimate the relative proportions of each cationic species formed. As can be seen from Figure 1 both β-carotenes are oxidized, along with a number of Chls. However, not only are the stoichiometries of these oxidation events difficult to estimate, but these relative quantities can themselves be variable according to sample preparation and excitation conditions (temperature, protein and acceptor concentration, intensity and length of illumination, etc.; not shown). Given that the absorption spectra are taken in different conditions to resonance Raman measurements (concentration, temperature, presence of glyc-

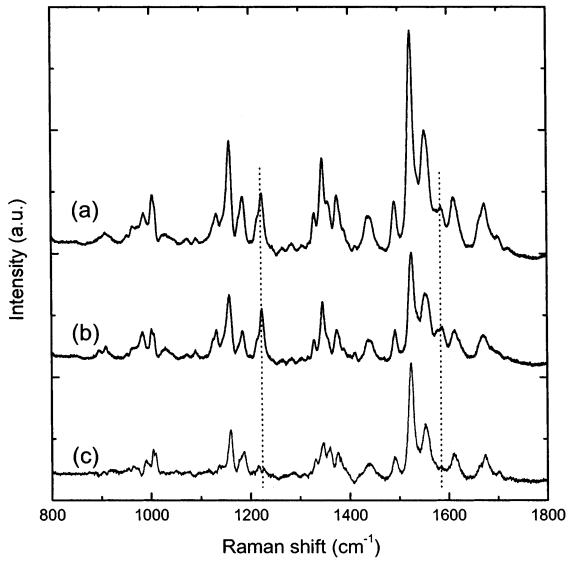

FIGURE 3: 413.1 nm excited resonance Raman spectra of RCII at 77 K after illumination in the absence (a) or presence (b) of SiMo, along with the corresponding difference spectrum (c). Dotted lines indicate the positions of modes unique to pheophytin, at 1224 and 1586 cm^{-1}.

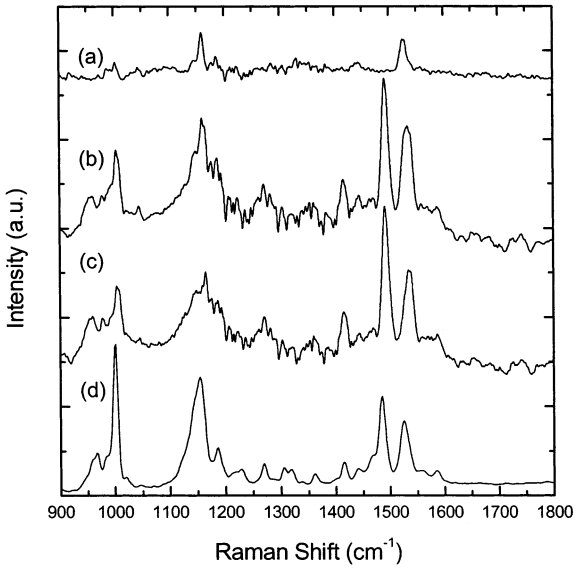

FIGURE 4: 840 nm excited resonance Raman spectra of RCII at 77 K after illumination in the absence (a) or presence (b) of SiMo. The corresponding difference spectrum (c) is also shown, along with the equivalent difference spectrum taken at 1064 nm excitation (d).

erol), a measure of these oxidation events for the Raman sample in situ is useful. As shown above, these two β-carotene molecules exhibit clear differences in the ν_3 region of their resonance Raman spectra, and excitation at 488.0 nm leads to similar contributions from each of them. Analysis of the light-induced changes in the ν_3 region using a 488.0 nm excitation thus allows for an estimation of the relative extent of oxidation of the two β-carotenes.

This comparison was performed for samples containing SiMo but which had not been exposed to a prior light treatment, using an excitation line weak enough so that its actinic effect (i.e., production of cations) was on a time scale longer than that of the measurement. A series of such spectra, corresponding to a progressive buildup of cationic species, indicated that Car_{507} and Car_{489} are oxidized to the same extent and at the same rate in our experimental conditions (data not shown, but cf. Figure 3c). Spectra from illuminated samples with or without SiMo may also be compared, provided that they can be normalized adequately. Normalization of the spectra in both intensity and frequency terms (for samples at the same concentration) was achieved using the band at 2326.6 cm^{-1}, which arises from the stretching modes of liquid N_2. Figure 3 displays Raman spectra of these preparations excited at 413.1 nm, conditions of resonance favoring contributions of Chl *a* and pheophytin molecules but also exciting modes of the two β-carotenes and the heme group of cytochrome b_{559}. These spectra therefore contain contributions from all of the pigments present in RCII. Spectra from illuminated samples with or without SiMo again indicate that both carotenoids are oxidized in these conditions, to approximately equal extents (Figure 3). The extent of oxidation is substantial (~50% of total Car) and greater than was seen in the absorption difference spectra (Figure 1). The low yield in the latter case is due to the presence of glycerol, required to form a glass, which strongly inhibits the electron acceptor efficiency of SiMo in PSII RCs at low temperature (Telfer and Schlodder, unpublished observations).

In the high-frequency region of these spectra (1640−1710 cm^{-1}), bands are observed arising from the conjugated carbonyl groups of the different chlorin molecules present (*47*, *50*, *51*, *57*). The position of these bands is sensitive both to the intermolecular interactions that these groups are involved in and to the dielectric constant of their local environment. These bands may shift by as much as 40 cm^{-1}, depending on the state of interaction of the conjugated carbonyl groups, and it is thus expected that their precise position will be different for each of the chlorin molecules present. In the difference spectrum (Figure 3c), this region contains contributions from at least three different modes, indicating that at least three different chlorin molecules are involved, contributing around 30% of the total area of the unbleached spectrum (Figure 3a). Note that it is possible, using the normalization protocol described above, to eliminate all bands corresponding to pheophytin and heme molecules (in particular, around 1224 and 1586 cm^{-1}; *50*, *57*), while this is not possible for any of the other molecular species present (data not shown). Thus, if any pheophytins have been bleached, it is only to a very small extent when compared to bleaching of the other pigments.

Excitation in the 800−850 nm region has previously been used to excite resonance Raman spectra of the PSII Chl cation, $Chl_Z^{+\bullet}$ (reviewed in *45*). However, contributions from $Car^{+\bullet}$ molecules present are also expected in such spectra due to post-resonance with their main transition around 990 nm (see Figure 1b). Presented in Figure 4 are Raman spectra of PSII reaction centers excited at 840 nm. Samples without an electron acceptor (i.e., unable to form stable Car and/or Chl cations) show only weak contributions located at 1527, 1159, and 1003 cm^{-1} (Figure 4a), matching the expected contributions of neutral carotenoid molecules (cf. Figure 2). This indicates that the enhancement of Chl modes in these conditions of excitation is very weak at best.

In illuminated samples containing SiMo (which therefore contain both Chl and Car cation species; see above), much more intense bands are observed (Figure 4b). The difference

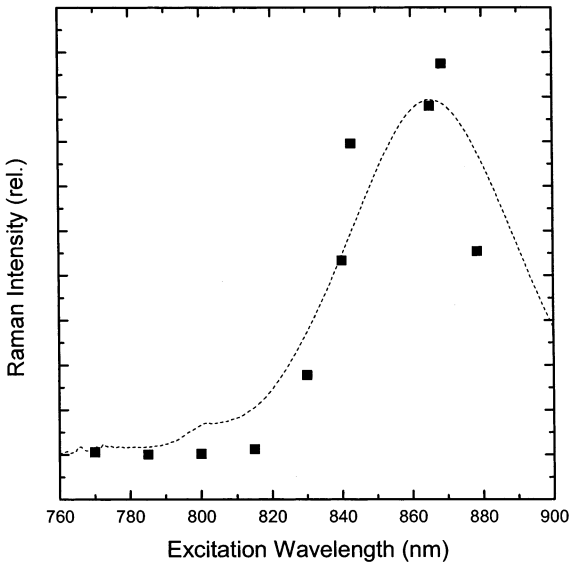

FIGURE 5: 77 K resonance excitation profile of the ~1490 cm^{-1} Raman band (see Figure 4), normalized to the liquid N_2 band at 2326.6 cm^{-1} (full symbols). Also shown (dashed line) is the cation-associated difference absorption spectrum (see Figure 1b), upshifted in energy by 1490 cm^{-1}.

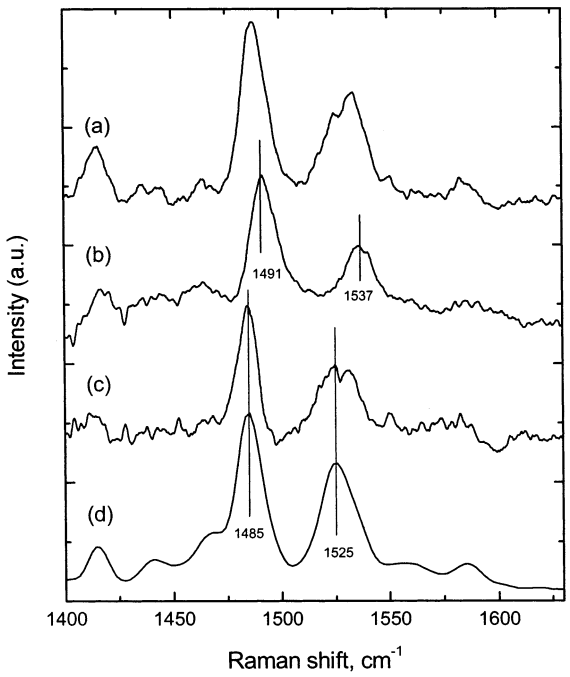

FIGURE 6: 77 K resonance Raman difference spectra of illumination-induced cations in RCII, at 870, 840, and 1064 nm excitation (a, b, and d, respectively; cf. Figure 4). A double-difference spectrum (c) was also calculated between spectra a and b, using an arbitrary normalization factor.

spectrum in Figure 4c exhibits modes which are all within the four characteristic regions associated with carotenoid species (ν_{1-4}; cf. Figure 2)—in particular, this spectrum is markedly similar to those of the $Car^{+\bullet}$ molecule as obtained by selective excitation close to its ~990 nm transition, at 1064 nm (Figure 4d; *42*, *43*). This is a strong indication that all of the major bands in this difference spectrum arise, at least in the main, from the carotenoid radical cation(s), $Car^{+\bullet}$. The two bands around 1490 and 1530 cm^{-1} (ν_1 region) are relatively very intense in these spectra, clearly more so than in those obtained at 1064 nm excitation (Figure 4d; *42*, *43*, *45*). The 840 nm excitation used in this experiment is located around 1500 cm^{-1} higher in energy than the ~990 nm transition. Additional intensity of bands in the 1500 cm^{-1} region could thus arise from resonance in 0−1 conditions. Indeed, particularly strong resonance of subsets of Raman bands may be observed when the excitation wavelength is located so that its difference in energy with the electronic transition of the molecule matches with the frequency of these modes (*58*). Such a mechanism could well be the origin of the higher intensity of the bands around 1500 cm^{-1} when using 840 nm excitation. It is of particular interest to note that no detectable bands could be observed at higher frequencies, where carbonyl vibrations of $Chl^{+\bullet}$ species are expected to contribute (*59*, *60*).

To test the possibility that these bands arise in 0−1 resonance conditions, we measured their excitation profile. Presented in Figure 5 is the integrated area of the ~1490 cm^{-1} band (where no significant contributions from neutral species are seen; Figure 4a), plotted as a function of the excitation wavelength (closed symbols). It was found that normalization to the 2326.6 cm^{-1} N_2 band was essential in this wavelength region, as the type of charge-coupled-device detector used in this work tends to lose sensitivity going into the near infrared, causing a blue-shift in the apparent profile before normalization (data not shown). Also plotted is the absorption envelope of the $Car^{+\bullet}$ molecules present (see Figure 1b), upshifted in energy by 1490 cm^{-1} (dashed line), and the comparison is quite striking given the difficulties expected in measuring such a profile. This represents fairly good evidence that the observed phenomenon is indeed due to 0−1 resonance with this ~990 nm transition, as mere post-resonance would give an increasing profile up into the absorption band.

Spectra excited throughout the range 800−900 nm gave results very similar to those shown in Figure 4. We therefore conclude that contributions of the $Car^{+\bullet}$ molecules present in the sample dominate the Raman spectra in excitation conditions above 800 nm, and that any bands corresponding to $Chl^{+\bullet}$ species are relatively smaller (e.g., Figures 4 and 6). It was, however, noted that the precise frequencies of the two bands around 1500 cm^{-1} varied with excitation wavelength. For example, in Figure 6 in spectra excited at 870 nm (Figure 6a), the position of these bands appears to be closer to those observed for 1064 nm excitation (i.e., 1485 and 1525 cm^{-1}). Shoulders at 1491 and 1537 cm^{-1} may, however, be observed in these spectra, corresponding to the main bands seen for 840 nm excitation (cf. Figure 6b). This phenomenon is even clearer in a difference spectrum between the two data sets (6a minus 6b), in which the normalization factor has been adjusted arbitrarily to minimize the bands observed at 840 nm excitation (Figure 6c). This difference is remarkably similar to the 1064 nm-excited $Car^{+\bullet}$ spectrum in this region (Figure 6d).

The shift in frequency of the 1500 cm^{-1} bands with excitation indicates that two different populations of carotenoid cation are contributing to the resonance Raman spectra, with slightly shifted excitation profiles (cf. refs *48* and *49*). Given that both Car_{507} and Car_{489} are oxidized in these conditions, it is very likely that the two sets of Raman bands correspond to these two β-carotene cations. Thus, the electronic transitions (and hence the 0−1 resonance excita-

tion profiles) of these two, nonequivalent $Car^{+\bullet}$ species are shifted relative to each other. It would seem a reasonable, if tentative, assumption that this absorption shift is the same as for their two neutral Car counterparts—i.e. that $Car_{507}^{+\bullet}$ absorbs at higher wavelengths than $Car_{489}^{+\bullet}$. Excitation at 840 nm would therefore be located in 0−1 resonance with the $Car_{489}^{+\bullet}$ electronic transition, with $Car_{507}^{+\bullet}$ modes becoming more dominant at higher wavelengths. Figure 6b would then represent "pure" $Car_{489}^{+\bullet}$, while the difference spectrum of Figure 6c (along with spectra excited at 1064 nm; Figure 5d, *42*, *45*) represents the contributions of "pure" $Car_{507}^{+\bullet}$. Thus, upon oxidation, the ν_1 of Car_{507} would be downshifted by 38 cm^{-1} (1523 cm^{-1} in Figure 2a to 1485 cm^{-1} in Figure 6c,d) and that of Car_{489} by 38.5 cm^{-1} (1529.5 cm^{-1} in Figure 2c to 1491 cm^{-1} in Figure 6b), remarkably similar values which would tend to confirm this assignment.

This large downshift in ν_1 upon Car oxidation has previously been interpreted as indicating that the hole on the $Car^{+\bullet}$ species in PSII is somewhat localized (*42*), based on an in vitro study of a range of other carotenoid cations (*61*). If this is genuinely the case then both $Car_{507}^{+\bullet}$ and $Car_{489}^{+\bullet}$ must exhibit this localization to the same extent. While a coincidence cannot be ruled out to explain this surprising observation, two other possibilities present themselves. It may be that this localization is necessary for some specific feature of the unusual function of these β-carotene molecules (such as the need to distance the positive charge from the P680 Chls in order to prevent reverse transfer). Alternatively, a ~40 cm^{-1} ν_1 downshift may in fact represent a β-carotene cation in which the hole is completely delocalized across the conjugated chain. We are currently taking measurements of a number of β-carotene analogues in their cation form in order to clarify this point. However, changes in both the conformation and configuration of these molecules upon in vitro oxidation are hard to avoid, and comparing such results with those observed in RCII may prove difficult.

The 1485 and 1491 cm^{-1} bands (Figure 6c,d for $Car_{507}^{+\bullet}$, and Figure 6b for $Car_{489}^{+\bullet}$, respectively) are of particular interest as a band in this region has previously been used as a "benchmark" for $Chl^{+\bullet}$ species (*34*), even though the 1485 cm^{-1} band has already been identified in 1064 nm-excited spectra as coming from $Car^{+\bullet}$ (*42*, *43*, *45*). Note that in shifted-excitation Raman difference spectroscopy (SERDS; *34*), a mode around 1485−1490 cm^{-1} is seen as an S-shaped feature centered at this frequency with a positive peak near 1480 cm^{-1}. Two lines of evidence were advanced for attributing this band to $Chl^{+\bullet}$. The first was the excitation profile of this mode, which appeared to follow the absorption spectrum of $Chl_Z^{+\bullet}$, peaking around 820−825 nm (*62*). In RCII preparations, we observe a band in the same position, but its excitation profile peaks somewhere around 860 nm (Figure 5, closed symbols), thus rather following 0−1 resonance conditions for the absorption bands of the two $Car^{+\bullet}$ species around 990 nm. The difference in excitation profiles between the present work and Cua et al. (*62*) could indicate that the contributions observed do not arise from similar species. However, this seems unlikely, given the similarity in the spectra in this region and the fact that $Chl^{+\bullet}$ species are also present here (Figures 1 and 3). On the contrary, most of the contributions observed in the spectra excited between 800 and 900 nm, including the "benchmark" feature previously assigned to $Chl_Z^{+\bullet}$ (*34*), match with those observed in spectra excited at 1064 nm, which are expected to contain pure $Car^{+\bullet}$ contributions (*42*, *45*; see Figures 4 and 5). It is possible that the observed differences in excitation profile reflect differences in absorption properties of the samples in each case. Variation in the relative stoichiometry of cations formed, as well as in the precise electronic properties of any one specific cation when formed, have already been observed between different experiments (e.g., refs *33* and *34*). These differences can be attributed to the particular organism and/or preparation used, or simply the illumination conditions (see above). Changes between the two sets of data in the $Car_{507}^{+\bullet}$: $Car_{489}^{+\bullet}$ ratio and/or in the precise absorption properties of each would result in an altered 0−1 resonance profile. Thus, the difference between 820 and 825 nm (*62*) and 840−870 nm in the present work is easily within the error range of Raman excitation profiles, which are themselves highly difficult to obtain with accuracy without very careful normalization.

The second line of argument used to attribute this feature to $Chl_Z^{+\bullet}$ involved the observed effect on it of mutations to the D1-H118 residue (*63*), which ligates the central Mg atom of $Chlz_{D1}$ (*15*). However, given that current structural models of PSII are not sufficiently accurate to locate either of the two β-carotene molecules, it is not possible to judge the effect of these mutations on spectra of any $Car^{+\bullet}$ species present. Small structural rearrangements around this residue as a result of the mutation could easily cause the perturbation of one or other carotenoid binding pocket, if it is close enough, and thus affect the Raman spectrum of this carotenoid in the neutral and/or cationic states. It should also be noted, in this regard, that spectroscopic and structural considerations with respect to the relative positions of the Chl_Z, Y_D, and cytochrome b_{559} cofactors have been used to place Chl_Z on the D2 rather than the D1 side of RCII (*15*, *64*, *65*)—i.e. at $Chlz_{D2}$ and not $Chlz_{D1}$ (*15*). Functional measurements on mutants exhibiting perturbations in each of these two binding sites are consistent with this alternative assignment (*66*, *67*).

Confirmation of the attribution of this mode to $Car^{+\bullet}$ comes from observation of its behavior in situations where the stoichiometry of the two cationic species varies in a known manner. It has been shown that in more intact PSII membrane preparations, 20 K illumination results principally in production of $Car^{+\bullet}$ with some $Chl_Z^{+\bullet}$ also being formed, while illumination at higher temperatures results in much lower $Car^{+\bullet}$ production, with the yield of $Chl_Z^{+\bullet}$ being higher (*33*). Warming of a sample containing $Car^{+\bullet}$ results in loss of the $Car^{+\bullet}$ species and a concomitant increase in $Chl_Z^{+\bullet}$ (*33*). In 1064 nm excited spectra of PSII membranes, the appearance and disappearance of this Raman band is seen to follow exactly that of the $Car^{+\bullet}$, and not the $Chl_Z^{+\bullet}$, species (Pascal et al., unpublished work). This observation supports the attribution of this mode to $Car^{+\bullet}$. Indeed, Tracewell et al. and Cua et al. observed a similar phenomenon in 820 nm excited SERDS spectra—the "benchmark" feature was seen upon illumination of PSII core preparations at 30 K, whereas it was lower for illuminations at increasing temperatures, closely following the yield of $Car^{+\bullet}$ rather than $Chl_Z^{+\bullet}$ (Figure 6 and Table 1 in ref *34*, Figure 2 in ref *62*).

The function of the two β-carotenes bound to photosystem II reaction centers is clearly different in many respects to

that of the carotenoids present in other photosynthetic proteins. These differences are in the main related to the difficulty of having oxidizable cofactors close to the highly oxidizing primary donor, P680. It is also extremely important to protect the system against a range of photoinhibitory events that may occur if the lifetime of its oxidized form, $P680^{+\bullet}$, is prolonged. One vital aspect of the function of these two β-carotenes appears to be their ability to reduce $P680^{+\bullet}$ in a relatively "inefficient" manner, as part of a secondary electron-transfer pathway(s?) around the periphery of PSII, in which Chl_Z and cytochrome b_{559} are also implicated. The importance of the two, spectroscopically distinct β-carotenes, their exact positioning within the three-dimensional structure, and the "sidedness" or otherwise of this pathway with respect to the D1 and D2 polypeptides are all subjects of ongoing investigation in a number of laboratories.

ACKNOWLEDGMENT

The authors would like to thank C. Büchel, K. Maghlaoui, J. Nield, and B. Hankamer for practical assistance as well as for many useful discussions.

SUPPORTING INFORMATION AVAILABLE

Resonance Raman spectra of RCII at 77 K after illumination in the presence of SiMo are shown for excitation at both 820 and 840 nm (cf. Figure 4), to allow for comparison with the 820 nm-excited spectra presented elsewhere (refs *34* and *62*). This material is available free of charge via the Internet at http://pubs.acs.org.

REFERENCES

1. Frank, H. A., and Cogdell, R. J. (1996) *Photochem. Photobiol. 63*, 257−264.
2. Frank, H. A., and Cogdell, R. J. (1987) *Biochim. Biophys. Acta 895*, 63−79.
3. Siefermann-Harms, D. (1985) *Biochim. Biophys. Acta 811*, 325−355.
4. Frank, H. A., and Cogdell, R. J. (1993) in *Carotenoids in Photosynthesis* (Young, A. J., and Britton, G., Eds.) pp 252−326, Chapman & Hall, London.
5. Ouchane, S., Picard, M., Vernotte, C., and Astier, C. (1997) *EMBO J. 16*, 4777−4787.
6. Arnoux, B., Ducruix, A., Reiss-Husson, F., Lutz, M., Norris, J., Schiffer, M., and Chang, C. H. (1989) *FEBS Lett. 258*, 47−50.
7. Kühlbrandt, W., Wang, D. N., and Fujiyoshi, Y. (1994) *Nature 367*, 614−21.
8. McDermott, G., Prince, S. M., Freer, A. A., Hawthornthwaite-Lawless, A. M., Papiz, M. Z., Cogdell, R. J., and Isaacs, N. W. (1995) *Nature 374*, 517−521.
9. Jordan, P., Fromme, P., Witt, H. T., Klukas, O., Saenger, W., and Krauss, N. (2001) *Nature 411*, 909−17.
10. Gounaris, K., Chapman, D. J., Booth, P., Crystall, B., Giorgi, L. B., Klug, D. R., Porter, G., and Barber, J. (1990) *FEBS Lett. 265*, 88−92.
11. Kobayashi, M., Maeda, H., Watanabe, T., Nakane, H., and Satoh, K. (1990) *FEBS Lett. 260*, 138−140.
12. Eijckelhoff, C., and Dekker, J. P. (1995) *Biochim. Biophys. Acta 1231*, 21−28.
13. Nanba, O., and Satoh, K. (1987) *Proc. Natl. Acad. Sci. U.S.A. 84*, 109−112.
14. Michel, H., and Deisenhofer, J. (1988) *Biochemistry 27*, 1−7.
15. Zouni, A., Witt, H. T., Kern, J., Fromme, P., Krauss, N., Saenger, W., and Orth, P. (2001) *Nature 409*, 739−43.
16. van Dorssen, R. J., Breton, J., Plijter, J. J., Satoh, K., van Gorkom, H. J., and Amesz, J. (1987) *Biochim. Biophys. Acta 893*, 267−274.
17. Breton, J., Duranton, J., and Satoh, K. (1988) in *Photosynthetic Light-harvesting Systems: Organization and Function* (Scheer, H., and Schneider, S., Eds.) pp 375−386, Walter de Gruyter, Berlin.
18. Kwa, S. L. S., Newell, W. R., van Grondelle, R., and Dekker, J. P. (1992) *Biochim. Biophys. Acta 1099*, 193−202.
19. Tomo, T., Mimuro, M., Iwaki, M., Kobayashi, M., Itoh, S., and Satoh, K. (1997) *Biochim. Biophys. Acta 1321*, 21−30.
20. Telfer, A. (2002) *Philos. Trans. R. Soc. London, Ser. B: Biol. Sci. 357*, 1431−1440.
21. Mimuro, M., Tomo, T., Nishimura, Y., Yamazaki, I., and Satoh, K. (1995) *Biochim. Biophys. Acta 1231*, 81−88.
22. Takahashi, Y., Hansson, Ö., Mathis, P., and Satoh, K. (1987) *Biochim. Biophys. Acta 893*, 49−59.
23. Durrant, J. R., Giorgi, L. B., Barber, J., Klug, D. R., and Porter, G. (1990) *Biochim. Biophys. Acta 1017*, 167−175.
24. Mathis, P., Satoh, K., and Hansson, O. (1989) *FEBS Lett. 251*, 241−244.
25. Barber, J., Chapman, D. J., and Telfer, A. (1987) *FEBS Lett. 220*, 67−73.
26. Barber, J. (1995) *Aust. J. Plant Physiol. 22*, 201−208.
27. Barber, J., and Andersson, B. (1992) *Trends Biochem. Sci. 17*, 61−66.
28. Telfer, A., Dhami, S., Bishop, S. M., Phillips, D., and Barber, J. (1994) *Biochemistry 33*, 14469−14474.
29. Klimov, V. V., and Krasnovskii, A. A. (1981) *Photosynthetica 15*, 592−609.
30. Watanabe, T., and Kobayashi, M. (1991) in *The Chlorophylls* (Scheer, H., Ed.) pp 287−315, CRC Press, Boca Raton, FL.
31. Edge, R., Land, E. J., McGarvey, D. J., Burke, M., and Truscott, T. G. (2000) *FEBS Lett. 471*, 125−127.
32. Bricker, T. M., and Ghanotakis, D. F. (1996) in *Oxygenic Photosynthesis: The Light Reactions* (Ort, D. R., and Yocum, C. F., Eds.) pp 113−136, Kluwer, Dordrecht, The Netherlands.
33. Hanley, J., Deligiannakis, Y., Pascal, A., Faller, P., and Rutherford, A. W. (1999) *Biochemistry 38*, 8189−95.
34. Tracewell, C. A., Cua, A., Stewart, D. H., Bocian, D. F., and Brudvig, G. W. (2001) *Biochemistry 40*, 193−203.
35. Telfer, A., De Las Rivas, J., and Barber, J. (1991) *Biochim. Biophys. Acta 1060*, 106−114.
36. Telfer, A., and Barber, J. (1995) in *Photosynthesis: From Light to Biosphere* (Mathis, P., Ed.) pp 15−20, Kluwer, Dordrecht, The Netherlands.
37. Moser, C. C., and Dutton, P. L. (1992) *Biochim. Biophys. Acta 1101* 171−176.
38. Thompson, L. K., and Brudvig, G. W. (1988) *Biochemistry 27*, 6653−8.
39. De Las Rivas, J., Telfer, A., and Barber, J. (1993) *Biochim. Biophys. Acta 1142*, 155−164.
40. Schenck, C. C., Diner, B., Mathis, P., and Satoh, K. (1982) *Biochim. Biophys. Acta 680*, 216−227.
41. Noguchi, T., Mitsuka, T., and Inoue, Y. (1994) *FEBS Lett. 356*, 179−182.
42. Pascal, A., Telfer, A., Barber, J., and Robert, B. (1999) *FEBS Lett. 453*, 11−4.
43. Vrettos, J. S., Stewart, D. H., de Paula, J. C., and Brudvig, G. W. (1999) *J. Phys. Chem. B 103*, 6403−6406.
44. Faller, P., Pascal, A., and Rutherford, A. W. (2001) *Biochemistry 40*, 6431−6440.
45. Tracewell, C. A., Vrettos, J. S., Bautista, J. A., Frank, H. A., and Brudvig, G. W. (2001) *Arch. Biochem. Biophys. 385*, 61−9.
46. Berthold, D. A., Babcock, G. T., and Yocum, C. F. (1981) *FEBS Lett. 134*, 231−234.
47. Noguchi, T., Tomo, T., and Inoue, Y. (1998) *Biochemistry 37*, 13614−13625.
48. Ruban, A. V., Pascal, A. A., and Robert, B. (2000) *FEBS Lett. 477*, 181−5.
49. Ruban, A. V., Pascal, A. A., Robert, B., and Horton, P. (2001) *J. Biol. Chem. 276*, 24862−70.
50. Ghanotakis, D. F., De Paula, J. C., Demetriou, D. M., Bowlby, N. R., Petersen, J., Babcock, G. T., and Yocum, C. F. (1989) *Biochim. Biophys. Acta 974*, 44−53.
51. Fujiwara, M., Hayashi, H., Tasumi, M., Kanaji, M., Koyama, Y., and Satoh, K. (1987) *Chem. Lett. 10*, 2005−8.
52. Bialek-Bylka, G. E., Tomo, K., Satoh, K., and Koyama, Y. (1995) *FEBS Lett. 363*, 137−140.

53. Yruela, I., Tomas, R., Sanjuan, M. L., Torrado, E., Aured, M., and Picorel, R. (1998) *Photochem. Photobiol. 68*, 729−737.
54. Koyama, Y., and Fujii, R. (1999) in *The photochemistry of carotenoids* (Frank, H. A., Young, A. J., Britton, G., and Cogdell, R. J., Eds.) pp 161−188. Kluwer, Dordrecht, The Netherlands.
55. Robert, B. (1999) in *The Photochemistry of Carotenoids* (Frank, H. A., Young, A. J., Britton, G., and Cogdell, R. J., Eds.) pp 189−201, Kluwer, Dordrecht, The Netherlands.
56. Pascal, A. A., Caron, L., Rousseau, B., Lapouge, K., Duval, J.-C., and Robert, B. (1998) *Biochemistry 37*, 2450−2457.
57. Moenne-Loccoz, P., Robert, B., and Lutz, M. (1989) *Biochemistry 28*, 3641−5.
58. Feiler, U., Albouy, D., Robert, B., and Mattioli, T. A. (1995) *Biochemistry 34*, 11099−11105.
59. Heald, R. L., and Cotton, T. M. (1990) *J. Phys. Chem. 94*, 3968−75.
60. Heald, R. L., Callahan, P. M., and Cotton, T. M. (1988) *J. Phys. Chem. 92*, 4820−4.
61. Jeevarajan, A. S., Kispert, L. D., Chumanov, G., Zhou, C., and Cotton, T. M. (1996) *Chem. Phys. Lett. 259*, 515−522.
62. Cua, A., Stewart, D. H., Brudvig, G. W., and Bocian, D. F. (1998) *J. Am. Chem. Soc. 120*, 4532−4533.
63. Stewart, D. H., Cua, A., Chisholm, D. A., Diner, B. A., Bocian, D. F., and Brudvig, G. W. (1998) *Biochemistry 37*, 10040−6.
64. Shigemori, K., Hara, H., Kawamori, A., and Akabori, K. (1998) *Biochim. Biophys. Acta 1363*, 187−198.
65. Rhee, K. H. (2001) *Annu. Rev. Biophys. Biomol. Struct. 30*, 307−28.
66. Ruffle, S. V., Wang, J., Johnston, H. G., Gustafson, T. L., Hutchison, R. S., Minagawa, J., Crofts, A., and Sayre, R. T. (2001) *Plant Physiol. 127*, 633−644.
67. Wang, J., Gosztola, D., Ruffle, S. V., Hemann, C., Seibert, M., Wasielewski, M. R., Hille, R., Gustafson, T. L., and Sayre, R. T. (2002) *Proc. Natl. Acad. Sci. U.S.A. 99*, 4091−4096.

BI026206P